Effect of Calcination Temperature on Structure of Mesoporous Borosilicate Bioglass

Effect of Calcination Temperature on Structure of Mesoporous Borosilicate Bioglass

S K Md Zain, E S Sazali*, F Mohd-Noor, S N S Yaacob

Advanced Optical Material Research Group, Department of Physics, Faculty of Science, Universiti Teknologi Malaysia, 81310 UTM Skudai, Johor, Malaysia.

Email: ezzasyuhada@utm.my

Abstract. Recently, most researchers have been focusing on the development of the mesoporous bioactive glasses for medical application. These materials are capable for bone tissue (soft and hard) regeneration and the delivery of bio-responsive active therapeutic molecules such as drug, proteins, nucleic acids, and peptides. However, the structure properties of the mesoporous bioactive glass are easily been controlled with a small change of calcination temperature during the sample preparation. In this perception, a series of mesoporous borosilicate bioactive glasses (MBBGs) with the composition of $10B_2O$ -$70SiO_2$ -15CaO- $5P_2O_5$ were prepared using the combination of sol-gel and evaporation induced self-assembly (EISA) and characterised. The calcination temperature of the bioactive glass preparation was controlled with varied temperature of 400°C, 500°C, 600°C and 700°C. The amorphous nature of the prepared samples were confirmed using XRD pattern. The EDX and FTIR spectra shows a small amount of carbon trapping inside the sample is increases with the increased of calcination temperature. All MBBGs samples show a ratio of Si-O-NBO and Si-O-Si (sym) bigger than 1. It is established that the structure of the mesoporous borosilicate bioactive glass can be tailored by controlling the calcination temperature.

1. Introduction

In the late 1960s, Larry Hench et al. developed new materials beside ceramic which is called bioactive glasses [1]. Compared to bioactive ceramic, bioactive glasses form a bond much faster. This is due to their dissolution of random amorphous network which is easier than crystalline ceramic, therefore hydroxycarbonate apatite (HCA) forms earlier on glass [2]. Fabrication of bioactive glass by sol gel with evaporation-induced self-assembly (EISA) technique resulting a mesoporous bioactive glass. Those mesoporous bioactive glasses exhibit a pore dimensions are within 2-50nm, which is resulting a superior bioactive property (formation of a HCA layer within a few hours) compared to bioactive glass made by traditional technique [3,4]. Several studies have been reported that borosilicate glass react quickly and convert more complexly to HCA compared to silicate 45S5 bioactive glass [5,6]. Xiu et. al has proved that mesoporous $CaO–B_2O_3–SiO_2$ glasses have a higher porosity and exhibit better in vitro bioactivity than conventional sol–gel-derived $CaO–B_2O_3–SiO_2$ glasses [7].

The mesoporous structure of the bioactive glass can be controlled by several ways. One of them by tuning the thermal condition of the mesoporous bioactive glass during the sample preparation. In 2017, Mariappan and Ranza have been investigated the effect of heat treatment on calcium phosphosilicate bioglass ceramics nanoparticles doped with silver [8]. They reported that no change of size and shape was clarified causes by the heat treatment but it shows better bioactivity and antibacterial properties against E. coli and S. aureus [8]. The studies on the effect of thermal treatment was continued by Vale

et al in 2019. On their studies, their found that the stabilization temperature of the AgBGs is around 510 °C, 100 °C/h+580 °C,½ h [9]. Cacciotti et. al also reported that, their 45S5 bioglass glass resulted in an amorphous behaviour with presence of cristobalite, calcium phosphate silicates crystal and carbon group with calcination temperature of 800ºC [10].

Recently, Delihta et. al studied on $80SiO_2$-$15CaO$-$5P_2O_5$ with different composition of Na. They found that the synthesis mesoporous bioactive glasses without additional Na prepared by 700ºC for 5h calcination condition exhibit in amorphous behaviour without any carbon entrapment [11]. However this calcination condition is not suitable when the MBG composition was added with Na. Only few works on introduction of boron in MBG have been reported. Two of them is work by Paul et. al [12] and Wu et. al [13] with MBG composition of 50Si-50B and $75SiO_2$-$15CaO$-$5P_2O_5$-$5B_2O_3$, respectively. Those two MBGs glasses have successfully been prepared with the different calculation condition. This proves that the change of glass composition needs a different calcination temperature. Therefore, the aim of this study is to determine the optimum calcination condition for mesoporous borosilicate bioglass with composition of $10B_2O_3$ –$70SiO_2$-$15CaO_2$-$5P_2O_5$. The effect of calcination condition on the mesoporous borosilicate bioglass behaviour can be explained more in term of their relation with other properties.

2. Experimental

A series of mesoporous borosilicate bioglass with composition of $10B_2O_3$ – $70SiO_2$-$15CaO_2$-$5P_2O_5$ with different calcination temperature such as 400ºC, 500ºC, 600ºC and 700ºC, have been prepared by EISA method. The mesoporous copper borosilicate bioglasses is synthesized by sol-gel method (using evaporation-induced self-assembly; EISA) as previous studies [14,15]. 8 g of P123 is dissolved in 120 g of ethanol followed by the addition of tetraethyl orthosilicate (TEOS, Si-precursor), boric acid (H_3BO_3) calcium nitrate tetrahydrate ($Ca(NO_3)_2.4H_2O$), copper nitrate ($Cu(NO_3)_2 \cdot 3H_2O$, and triethylphosphate (TEP) at room temperature under fume hood. The mixture is vigorously stirred for 7 hours, then transfered into petri dish and kept at 35ºC under fume hood for evaporation- induced self-assembly (EISA) process. After 1 day of EISA process, the gel sample is aged at 60ºC for another day. Then the glass was be separated into a several part and applied in different thermal treatments of calcination process (400ºC, 500ºC, 600ºC and 700ºC). The amorphous nature of mesoporous borosilicate bioglasses (MBBGs) is confirmed by X-ray diffraction pattern from Rigaku SmartLab High Resolution X-Ray Diffractometer equipped with CuKα radiation with wavelength 1.5406 Å in the 2Θ range of 10-60 and 0.02 step size. The structural properties of MCBBG have be tested by Fouri Transform Infrared (FTIR). The FTIR spectra have been found by pellet the sample with KBr with the ratio of 1:100 and 4 cm^{-1} resolution.

3. Results and discussions

The mesoporous borosilicate bioactive glass (MBBG) samples with composition of $10B_2O_3$ – $70SiO_2$-$15CaO_2$-$5P_2O_5$ have been prepared by sol-gel and EISA method with different calcination temperature such as 400ºC, 500ºC, 600ºC and 700ºC. Samples with different calcination condition of 400ºC, 500ºC, 600ºC and 700ºC are naming as S400, S500, S600 and S700, respectively. Figure 1 depicted the X-ray diffraction pattern for S400, S500, S600 and S700 samples. It is apparent that, a common diffusion halo is present in the XRD pattern in the range of 20-35 degree, which confers the amorphous nature [16] and short range structural disorder of the glasses [17]. From Figure 1, it also can be seen that there are absent of sharp peak in the XRD pattern, this verify that the structure of glass does not appearance any crystal.

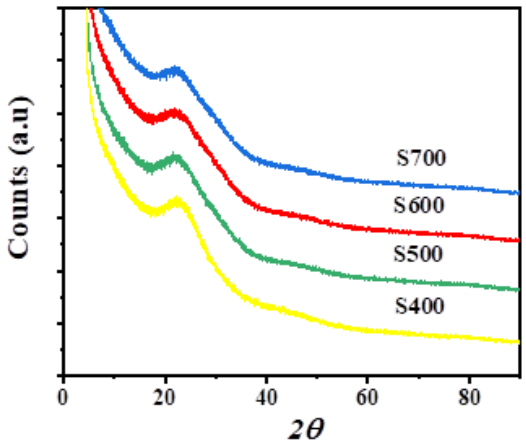

Figure 1. The X-ray diffraction pattern of S400, S500, S600 and S700 samples with different calcination condition.

In order to confirm the present of element in the MBBG, the Energy Dispersive X-ray (EDX) spectroscopy was used. Elemental Analysis of MBBG determined by EDX Spectroscopy, the result from all samples (S400, S500, S600 and S700) are listed in table 1. The element analysis are in the range of 47.0 to 51.2, 28.1 to 30.7, 11.6 to 8.5,0.8 to 1.7, 1.4 to 2.2, and 5.9 to11.0 for O, Si, Ca, P, B and C element, respectively. Besides O element, Si element also? shows a higher weight percentage compared to other element due to the higher amount of TEOS used during the sample preparation compared to other raw material. From table 1, it is clearly seen that, the increment of calcination temperature reduces the weight percentage of the Si, Ca, P, and B element. This indicates that the change of calcination temperature may affect the present of element inside the glass network. On the other hand, the weight percentage of C element is increased with the increase of calcination temperature. One reason for the increment might be due to the carbon trapping inside the glass structure during the calcination process.

Table 1: Elemental Analysis of MBBG

Element	S400	S500	S600	S700
O	51.2	50.9	48.7	47
Si	30.7	29.6	28.3	28.1
Ca	8.5	9.9	11.6	10.7
P	1.5	1.1	0.8	1.7
B	2.2	2.1	1.4	1.5
C	5.9	6.4	9.2	11.0

Nitrogen (N_2) adsorption-desorption isotherms are used to determine the mesoporosity and surface area of samples. Figure 2 shows the Nitrogen adsorption-desorption isotherms of MBBG with three different calcination temperatures. Sample S400, S500, S600 and S700 exhibit typical type IV isotherms and hysteresis loops are type 1, which indicate the presence of hexagonal *p6nm* mesoporous [5]. From those figure sample S700 shows small N_2 absorbed volume (weak step), which attributed to the irregular pore structure [18]. The calculated data of the BET surface area, pore volume and pore size of MBBG samples are listed in table 2. The S600 had the highest surface area and pore volume of 388.6 m^2g^{-1} and 0.66cm^3g^{-1}, respectively, which higher compared to previous studies [19] [14]. It can also be found that the surface area and pore volume S700 is small compared to S400, S500 and S600. This significant difference of surface area and pore volume may result by difference ordered degree of sample. The S700 with 700^{o}C calcination temperature might causes a carbon trapping inside the glass network. The pore distribution curve was analysed from the N2 desorption branches using the BJH model (Figure 3). The BJH pore size distribution curve indicates that, all samples S400, S500, S600 and S700 have a narrow size of pores around 2.0 and 2.9 nm, respectively.

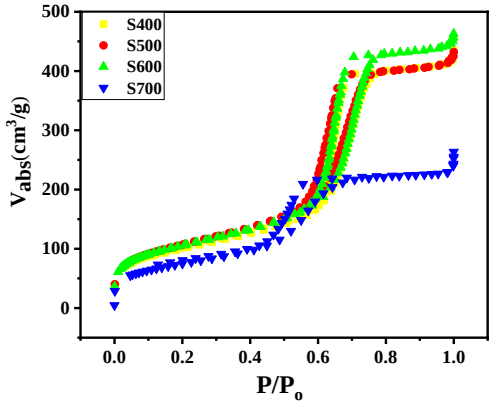

Figure 2: Nitrogen adsorption-desorption isotherms of MBBG.

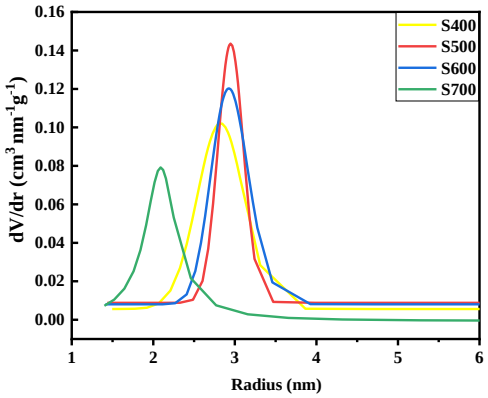

Figure 3: The BJH pore size distribution curve.

Table 2 : Textural parameter of MBBG.

Sample	BET Surface Area (±0.1 m^2/g)	Pore Volume (±0.01cm^3/g)	Pore Size (±0.01nm)
S400	375.6	0.69	2.91
S500	370.7	0.65	2.92
S600	388.6	0.66	2.76
S700	269.3	0.39	2.09

Figure 2 shows the FTIR spectra of all MBBG samples with different calcination temperature. Each of the spectra is deconvoluted in the range of 400- 2000 cm^{-1} wavenumber as shown in Figure 3. The moderate band around 1648 cm^{-1} is attributed to the stretching vibration of the H-O bond of H_2O that was absorbed in the materials or silanol group (Si-O-H). The Gaussian shape are consistent in all sample and had been assigned as listed in table 3. It can be seen that, the area of carbonate band near 1390-1430 cm^{-1} is increased with the increase of temperature, which might be due to carbon trapping inside the sample [20]. This result is agreement with pervious result in EDX analysis, which assigned the carbon contain is increased with the increment of calcination temperature.

Basically, the unit of silicate tetrahedral is participating and linking with four bridging oxygen to neighbouring silicon atoms. The present of network modifiers ($B^{3+}$and Ca^{2+}) in the glass structure can provoke the destruction of the glass network continuity by breaking the Si-O-Si bond. Commonly, the unit of silicate tetrahedral are donated as Q^n, where n refer to the number of bridging respectively possess by four, three, two and one non-bridging oxygen atom [21]. From figure 5 the vibration mode of Si-O-NBO and symmetric stretching mode of Si-O-Si is a characteristic of Q^3 and Q^4 group. According to Ma.J in 2010, the relative ratio between Q^3 and Q^4 group can be used to show the polymerization degree of the synthesized glass [22]. Figure 6, show the intensity ratio of Q^3 and Q^4 for MBBG sample as a function of calcination temperature. The value of ratio is increases from 2.61 to 2.99 and then it slightly decreases to 2.79 when the sample is heat with 700°C in the calcination process. This is indicated that the sample S600 with 600°C calcination temperature show a higher intensity ratio of Q^3 and Q^4. Previous studies by Serra J. et. al have reported that, sample with ratio of Q^3 and Q^4 bigger than 1 have a higher potential as bioactive material [23]. This is due to the efficient ion exchange, dissolution pf silicate and formation of HCA layer on the glass surface. Therefore, compared to the previous studies, all the synthesized glasses have a bigger ratio.

Table 3 : The assignment of different vibrational band from FTIR spectra of samples.

Wavenumber (cm^{-1})				Assignments	Reference
S400	**S500**	**S600**	**S700**		
466	464	466	464	Rocking motion of Si-O-Si units	[8]
569	575	577	579	Bending mode of P-O (crystalline phosphate)	[20]
792	793	793	796	Si-O-Si symmetric stretching mode	[24]
931	932	930	930	Vibration mode of Si-O-NBO	[8,7]
1072	1073	1071	1075	Si-O-Si asymmetric stretching of bridging oxygen atoms within the tetrahedron	[25 , 26]
1212	1213	1213	1223	Vibrational mode of asymmetric stretch Si–O–Si	[27 , 28]
1323	1323	1327	1319	Asymmetric stretching mode of BO_2O-	[29]
1429	1433	1416	1393	Carbonate bands	[20]
1488	1511	1490	1482	Asymmetric stretching mode of BO	[29]
1648	1649	1648	1649	Stretching vibration of the H - O bond of H_2O	[30 , 20]

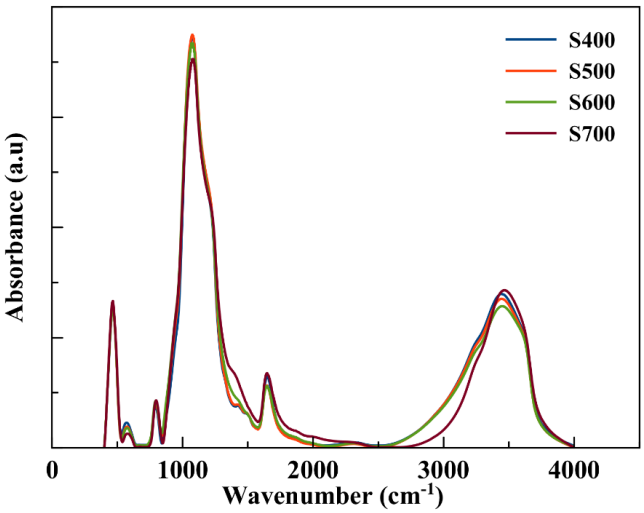

Figure 4 : The FTIR spectra of the MBBG with different calcination condition.

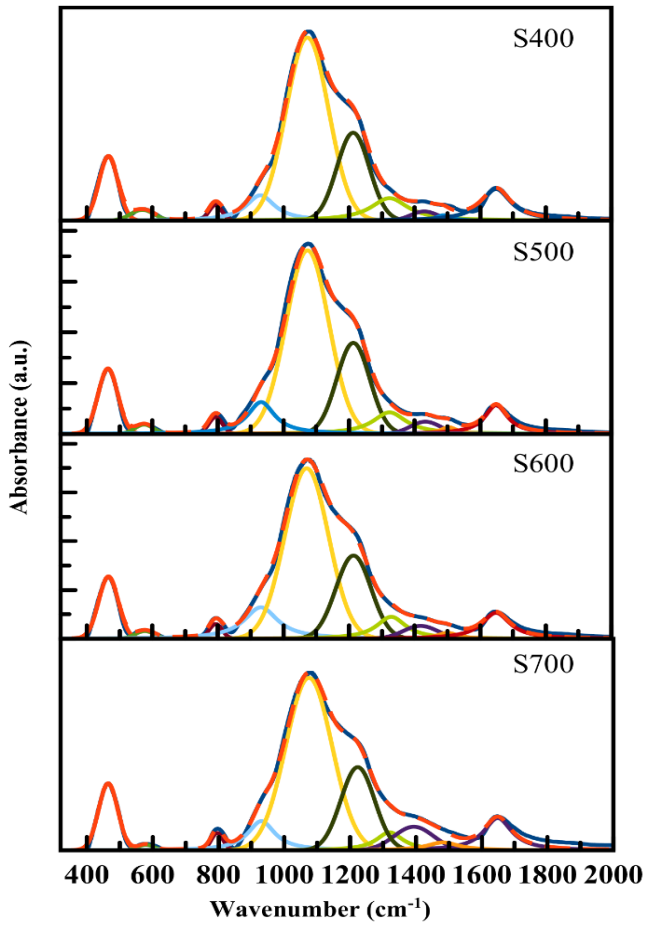

Figure 5 : Deconvoluted FTIR spectra of the bioactive glasses for MBBG samples.

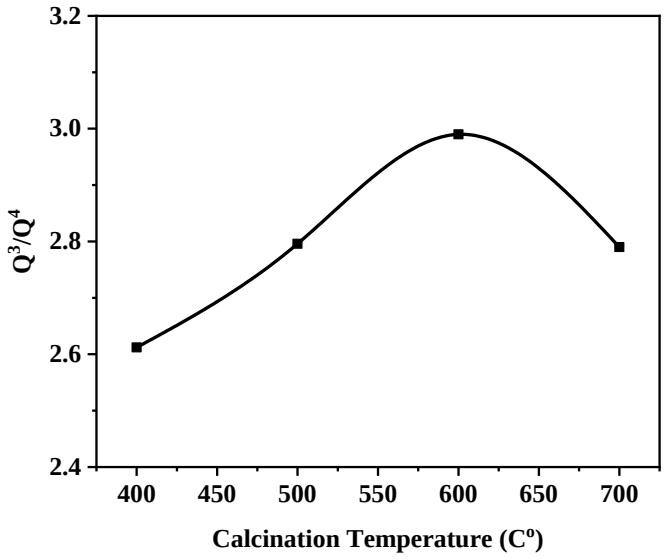

Figure 6: Ratio of Si-O-NBO and Si-O-Si (sym) against calcination temperature of samples.

4. Conclusion

Mesoporous borosilicate bioactive glass with different calcination temperatures have been prepared by the EISA method. The influence of calcination temperature in MBBG can be observed clearly on the morphology and structural. The results from Nitrogen adsorption-desorption isotherms reveal that all glasses possess high specific surface area and porous volume, they are influenced by the difference calcination temperature. Besides that, calcination temperature also resulted in the element contain inside the glass network, where the carbon contain is increasds with the increment of calcination temperature. In addition, with increasing of calcination temperature, decreased of perturbation of the silica network is found and the variations of Si–O–NBO(Q3)/Si–O(s, sym)(Q4) absorbance intensity ratio are increased from 2.61 to 2.99.

Acknowledgements

The authors acknowledge the Research University Grant (Vote:01M39 and 18J93) and the Public Service Department Malaysia for the financial support. Thanks, and appreciations are extended to the laboratory technical staff of Physics Department, UTM for their constant cooperation and support.

References

[1] Baino F, Fiorilli S and Vitale-brovarone C 2016 Acta Biomaterialia Bioactive glass-based materials with hierarchical porosity for medical applications : Review of recent advances *Acta Biomater.* **42** 18–32

[2] Sultana N 2013 Scaffolds for Tissue Engineering *SpringerBriefs in Applied Sciences and Technology* pp 1–17

[3] Izquierdo-Barba I and Vallet-Regí M 2015 Mesoporous bioactive glasses: Relevance of their porous structure compared to that of classical bioglasses *Biomed. Glas.* **1** 140–50

[4] Kargozar S, Lotfibakhshaiesh N, Ai J, Mozafari M, Brouki P, Hamzehlou S, Barati M, Baino F, Hill R G and Taghi M 2017 Acta Biomaterialia Strontium- and cobalt-substituted bioactive glasses seeded with human umbilical cord perivascular cells to promote bone regeneration via enhanced osteogenic and angiogenic activities *Acta Biomater.* **58** 502–14

[5] Haro Durand L A, Vargas G E, Romero N M, Vera-Mesones R, Porto-López J M, Boccaccini A R, Zago M P, Baldi A and Gorustovich A 2015 Angiogenic effects of ionic dissolution products released from a boron-doped 45S5 bioactive glass *J. Mater. Chem. B* **3** 1142–8

[6] Gustavo R, Wagner F, Correr R, Flavia A, Russi C, Rosas M, Trovatti E and Pecoraro É 2018 Preparation and characterization of boron-based bioglass by sol − gel process *J. Sol-Gel Sci. Technol.* 181–91

[7] Xiu T, Liu Q and Wang J 2008 Comparisons between surfactant-templated mesoporous and conventional sol-gel-derived CaO-B2O3-SiO2 glasses: Compositional, textural and in vitro bioactive properties *J. Solid State Chem.* **181** 863–70

[8] Mariappan C R and Ranga N 2017 Influence of silver on the structure, dielectric and antibacterial effect of silver doped bioglass-ceramic nanoparticles *Ceram. Int.* **43** 2196–201

[9] Vale A C, Pereira P R, Barbosa A M, Torrado E and Alves N M 2019 Materials Science & Engineering C Optimization of silver-containing bioglass nanoparticles envisaging biomedical applications *Mater. Sci. Eng. C* **94** 161–8

[10] Cacciotti I, Lombardi M, Bianco A, Ravaglioli A and Montanaro L 2012 Sol–gel derived 45S5 bioglass: synthesis, microstructural evolution and thermal behaviour *J. Mater. Sci. Mater. Med.* **23** 1849–66

[11] Delihta J, Fernando L, Delihta J, Fernando L, Mesoporous N and Glasses B 2018 Novel Mesoporous Bioactive Glasses (MBGs) as fillers in dental adhesives " Synthesis , Physico-chemical and biological evaluation " To cite this version : HAL Id : tel-01943600 Novel Mesoporous Bioactive Glasses (MBGs) as fillers in dental adhesives « *Biomaterials*

[12] Paul M, Pal N and Bhaumik A 2012 Selective adsorption and release of cationic organic dye

molecules on mesoporous borosilicates *Mater. Sci. Eng. C* **32** 1461–8
[13] Nanofibers B G 2011 Preparation and In Vitro Bioactivity of Novel Mesoporous Borosilicate Bioactive Glass Nanofibers **2845** 2841–5
[14] Zhu Y, Li X, Yang J, Wang S, Gao H and Hanagata N 2011 Composition-structure-property relationships of the CaO-MxO y-SiO2-P2O5 (M = Zr, Mg, Sr) mesoporous bioactive glass (MBG) scaffolds *J. Mater. Chem.* **21** 9208–18
[15] Wu C, Miron R, Sculean A, Kaskel S, Doert T and Schulze R 2011 Proliferation , differentiation and gene expression of osteoblasts in boron-containing associated with dexamethasone deliver from mesoporous bioactive glass scaffolds *Biomaterials* **32** 7068–78
[16] Anand A, Lalzawmliana V, Kumar V, Das P, Devi K B, Maji A K, Kundu B, Roy M and Nandi S K 2019 Preparation and in vivo biocompatibility studies of different mesoporous bioactive glasses *J. Mech. Behav. Biomed. Mater.* **89** 89–98
[17] Hajer S S, Halimah M K, Zakaria A and Azlan M N 2016 Effect of Samarium Nanoparticles on Optical Properties of Zinc Borotellurite Glass System *Mater. Sci. Forum* **846** 63–8
[18] Rani J, Song Y and Yang Y 2018 The in fl uence of isothermal aging , surfactant and inorganic precursors concentrations on pore size and structural order of mesoporous bioactive glass *Solid State Sci.* **84** 104–11
[19] Zhang X, Zeng D, Li N, Wen J, Jiang X, Liu C and Li Y 2016 Functionalized mesoporous bioactive glass scaffolds for enhanced bone tissue regeneration *Sci. Rep.* **6** 1–12
[20] Anand A, Lalzawmliana V, Kumar V, Das P and Devi K B 2019 Journal of the Mechanical Behavior of Biomedical Materials Preparation and in vivo biocompatibility studies of di ff erent mesoporous bioactive glasses *J. Mech. Behav. Biomed. Mater.* **89** 89–98
[21] Habasaki J 2019 Heterogeneous–homogeneous transition and anomaly of density in SPC/E water examined by molecular dynamics simulations *Phys. A Stat. Mech. its Appl.* **527**
[22] Ma J, Chen C Z, Wang D G and Shi J Z 2010 Textural and structural studies of sol-gel derived SiO2-CaO- P2O5-MgO glasses by substitution of MgO for CaO *Mater. Sci. Eng. C* **30** 886–90
[23] Serra J, González P, Liste S, Chiussi S, León B, Pérez-Amor M, Ylänen H O and Hupa M 2002 Influence of the non-bridging oxygen groups on the bioactivity of silicate glasses *J. Mater. Sci. Mater. Med.* **13** 1221–5
[24] Gargiulo N, Cusano A M, Causa F, Caputo D and Netti P A 2013 Silver-containing mesoporous bioactive glass with improved antibacterial properties *J. Mater. Sci. Mater. Med.* **24** 2129–35
[25] Kumar A, Mariappan C R and Sarahan B S 2019 Antibacterial and structural properties of mesoporous Ag doped calcium borosilicate glass-ceramics synthesized via a sol-gel route *J. Non. Cryst. Solids* **505** 431–7
[26] Anand A, Kundu B, Balla V K, Nandi S K, Anand A, Kundu B, Balla V K and Nandi S K 2018 Transactions of the Indian Ceramic Society Synthesis and Physico-Chemical Characterization of Different Mesoporous Bioactive Glass Nanopowders : in-vitro SBF Activity and Cytotoxicity Synthesis and Physico-Chemical Characterization of Different Mesoporous **5456**
[27] Kumar A, Sudipta and Murugavel S 2020 Influence of textural characteristics on biomineralization behavior of mesoporous SiO2-P2O5-CaO bioactive glass and glass-ceramics *Mater. Chem. Phys.* **242** 122511
[28] Izquierdo-Barba I, Ruiz-González L, Doadrio J C, González-Calbet J M and Vallet-Regí M 2005 Tissue regeneration: A new property of mesoporous materials *Solid State Sci.* **7** 983–9
[29] Lai Y, Zeng Y, Tang X, Zhang H, Han J and Su H 2016 Structural investigation of calcium borosilicate glasses with varying Si/Ca ratios by infrared and Raman spectroscopy *RSC Adv.* **6** 93722–8
[30] Mubina M S K, Shailajha S, Sankaranarayanan R and Saranya L 2019 In vitro bioactivity, mechanical behavior and antibacterial properties of mesoporous SiO2-CaO-Na2O-P2O5 nano bioactive glass ceramics *J. Mech. Behav. Biomed. Mater.* **100** 103379